Materials Science Forum Vols. 299-300 (1999) pp 70-79

doi:10.4028/www.scientific.net/MSF.299-300.70

Synthesis of Zirconia-based Solid Electrolyte Powders by the Coprecipitation Technique

E.N.S. Muccillo, R. Muccillo and D.M. Ávila

Instituto de Pesquisas Energéticas e Nucleares, Comissão Nacional de Energia Nuclear, C. P. 11049, Pinheiros, S. Paulo, SP, 05422-970, Brazil

Keywords: Synthesis, Coprecipitation, Zirconia

Abstract. The coprecipitation technique has been used in order to obtain zirconia-magnesia and zirconia-ceria powders with suitable purity and sinterability, respectively. To accomplish those requests, some processing variables have been systematic studied and optimized. Similar solid solutions have been prepared by the powder mixing technique for comparison purposes. Inductively coupled plasma, thermal neutron activation, nitrogen adsorption/desorption, thermal analyses and scanning electron microscopy techniques have been used for powder characterization. Cylindrical pellets were prepared by uniaxial and cold isostatic pressing. The characterization of the sintered pellets have been carried out by impedance spectroscopy, scanning electron microscopy and X-ray diffraction techniques. Zirconia-magnesia ceramics with a high degree of purity have been obtained., in agreement with impedance spectroscopy results that show no grain boundary blocking effects. For the zirconia-ceria system, sintered pellets with 98% of the theoretical density, and 0.5 μm average grain size have been obtained without using any comminution or special drying processes.

Introduction

Several techniques have been used for processing zirconia-based ceramics. Solid-phase methods are the conventional routes based on solid state reactions. They involve several steps and, in general, they are not able to yield homogeneous distribution of low-level additives when they are required. Moreover, the mixing and milling operations can also introduce unwanted impurities. Chemical synthesis techniques have been developed to overcome the limitations of conventional powder preparation methods. Vapor-phase methods, on the other hand, have higher costs in comparison with solution-phase methods. Precipitation or coprecipitation is one of the oldest and most used solution-phase methods, both in laboratory scale and industrial scale [1]. Compared with other chemical techniques it offers several advantages like increase in solid solution formation rate, and the possibility to obtain metastable phases at room temperature [2]. In addition, powders prepared by this technique present improved chemical homogeneity and high values of specific surface area, which result in reduced temperature and/or time for sintering. Besides its operational simplicity, the coprecipitation technique involves a number of variables that should be controlled for processing reproducibility. These processing variables influence the microstructure of the sintered ceramic thereby affecting their microstructure-related properties.

There are relatively few works dealing with the effect of optimization of these variables on the microstructure of the sintered ceramic. Some results in the literature indicate that the cation solution concentration governs the precipitate morphology. It was also observed [3] a reduction in the sintered density for increasing concentration of the cation solution. The precipitant agent solution concentration has several effects on the precipitate. For Mg-doped zirconia it has been shown that it reduces the anion content in the gel, the crystallization temperature, and the initial temperature for the tetragonal to monoclinic martensite phase transformation [4]. In the case of solid solution synthesis, it is usual to perform the process by adding the cation solution to the precipitant solution.

This procedure avoids segregation effects when the initial precipitation pH of the cations are quite different. The phase assemblage after calcination and the average crystal size are also defined by this variable. Less studied was the effect of precipitation temperature. It was recently shown [5] that for a fixed pH value there is an increase in the monoclinic phase fraction along with a reduction in the average crystal size with the increase of the precipitation temperature. One of the most studied processing variables is the washing medium because it controls the agglomeration state of the precipitate [6-9]. An additional step of washing with organic liquids is usually employed giving rise to a gel with soft agglomerates. Finally, the calcination of the dried powder must be scheduled in such a way that it allows for crystallization along with minor reduction in the value of specific surface area. Although different processing conditions result in structural differences, many of these are lost during sintering [10]. However, to obtain improved microstructure in the sintered ceramics these processing variables should be studied and modified according to the type and concentration of the cations.

In this work some of these variables have been systematic studied in order to obtain zirconia-magnesia and zirconia-ceria powders with suitable purity and sinterability, respectively.

Experimental

Synthesis of ZrO_2: MgO

A 1 M $MgCl_2.6\ H_2O$ (P. A., Ecibra) solution was added to a 0.6 M $ZrOCl_2.8\ H_2O$ (99%, Vetec) solution. The relative concentration of the magnesium chloride solution was adjusted to give, approximately, 13 mol% MgO in the calcined powder. The mixed solution was added at a rate of 50 $mL.min^{-1}$ to a previously determined amount of 6 M NH_4OH precipitant solution under vigorous stirring. The final pH value was 10-11. This value corresponds to the pH of the supernatant liquid. In order to keep this pH value constant throughout this step a 1 M NH_4OH solution was added when necessary. The reagents used were of analytical grade. The resulting gelatinous precipitate was dispersed in distilled water (300 mL for each 50 mL of initial zirconyl chloride solution), and collected by vacuum filtration. This washing cycle was repeated four times. At this point, test for Cl^- with a 1 M $AgNO_3$ solution was performed in the usual manner. The precipitate was then washed twice with ethanol, ultrasonically dispersed for 10 min, and washed once again with ethanol. Samples were dried at room temperature in a dessicator and calcined at 850 °C / 1 h. Cylindrical pellets have been prepared by uniaxial and cold isostatic pressing. Sintering has been carried out at 1450 °C / 2 h followed by 1700 °C / 1 h in air.

For comparison purposes, specimens of the same composition were prepared by the powder mixing technique. ZrO_2 (DK-2 type, Zirconia Sales) and MgO (99.9%, P. A., Merck) were wet mixed and dried. The mixtures were pressed and sintered at 1650 °C/2 h.

Synthesis of ZrO_2: CeO_2

$ZrOCl_2.8\ H_2O$ (99.9%, BDH) and $Ce(NO_3)_3.6\ H_2O$ (> 99.5%, IPEN) were used as starting materials. Fig. 1 shows the flow chart of the experimental sequence. The aqueous cation solution was added to a precipitant solution under stirring. The resultant precipitate was submitted to a washing cycle, dried and calcined. Some variables have been studied in this case. The precipitant solution concentration was varied between 1 M and 9 M. Washing was performed in water followed by ethanol, or in a diluted ammonia solution and ethanol. The effect of digestion of the precipitate on the morphology of the calcined powder has also been followed. Calcination temperature and time were chosen from results of thermogravimetric analysis and sintered density, respectively. Other processing variables were fixed according to previous results. All precipitation experiments have been done at a pH value of 10 at room temperature. The precipitate was dried in air at 45 °C for 24

h. Nominal concentration of ceria was 12 mol%. Pellets have been prepared by uniaxial and cold isostatic pressing. Sintering has been carried out at 1500 °C / 2 h.

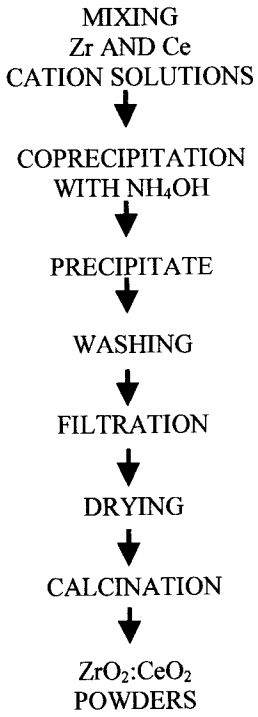

Fig. 1: Experimental sequence for synthesis of zirconia-ceria.

Characterizations

Powder analyses comprise: impurity contents by inductively coupled plasma, dopant content by neutron activation, anion content by pyrohydrolisis, specific surface area by nitrogen adsorption/desorption, mass loss by thermogravimetric analysis, and powder morphology by electron microscopy techniques. Linear shrinkage has been followed using a Netzsch dilatometer model 402 E/7. The characterizations of the sintered pellets have been carried out by X-ray diffraction (Philips X'Pert) using a Ni filtered Cu K_α radiation. Apparent densities have been determined by the water displacement method. Fractured or polished and thermally etched surfaces of pellets have been observed by scanning electron ,microscopy (JXA 6400 Jeol, XL30 Philips). Impedance spectroscopy have been carried out by an HP 4192A LF impedance analyzer in the 300 °C – 550 °C temperature range using Ag or Pt as electrode material.

Results and Discussion

Zirconia-Magnesia. Table 1 shows impurity content for commercial zirconia (DK-2) and coprecipitated zirconia-magnesia (ZM) precursor powders. It is worth to note the relative low silicon and aluminum impurity contents in the coprecipitated material.

Table 1: Metallic impurity content (in wt.%) determined by inductively coupled plasma.

ELEMENT	ZM	DK-2
Fe	< 0.0075	0.0015
P	< 0.15	0.04
Si	0.02	0.04
Al	< 0.006	0.01
Na	-	0.003
Ca	0.01	-

An average particle size of approximately 0.8 μm for the calcined coprecipitated powder was estimated from TEM observations.

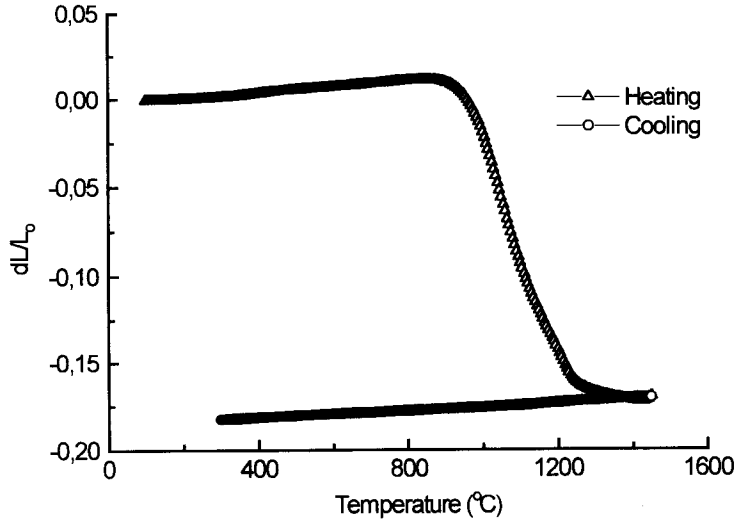

Fig. 2: Dilatometry curve of the zirconia-magnesia prepared by the coprecipitation technique.

Values of specific surface area for DK-2 and MgO powders are 3.4 and 34.5 $m^2.g^{-1}$, respectively.

Fig. 2 shows the result of dilatometry for the specimen prepared by the coprecipitation technique. Retraction occurred between 900 °C and 1300 °C and total shrinkage was 185. This shows that densification was accomplished during the first thermal treatment at 1450 °C, while during the post sintering heat treatment at 1700 °C grain growth was enhanced.

Sintered densities and magnesium content are shown in Table 2. These relative low values of densities are mainly due to a high fraction of closed porosity normally found in cubic zirconias. Despite minor differences resulting from an heterogeneous distribution of the stabilizer, both powders have similar chemical composition as shown by neutron activation analysis.

Table 2: Sintered densities (d_s) measured by the hydrostatic technique and MgO content determined by thermal neutron activation analysis of specimens.

SYNTHESIS TECHNIQUE	d_s ($g.cm^{-3}$)	MgO content (mol%)
Coprecipitation	4.90	13.1
Powder mixing	5.07	13.0

Fig. 3: shows a scanning electron microscopy (SEM) micrograph of a fractured surface of the coprecipitated specimen. The predominant mode of fracture is transgranular with a high fraction of closed porosity as expected from density results. Fig. 4 is a SEM micrograph of the polished and thermally etched surface of the specimen prepared by the powder mixing technique. An average grain size of 20 μm along with extensive porosity are observed.

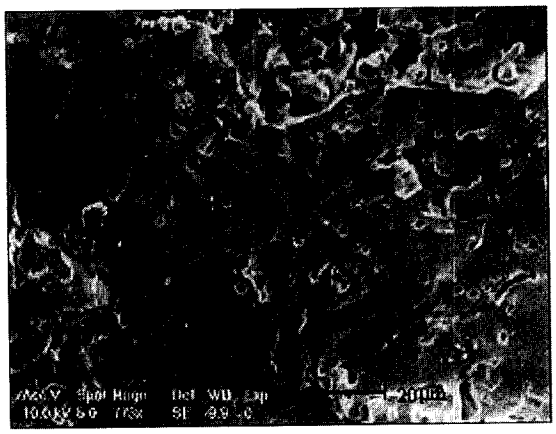

Fig. 3:SEM micrograph of a fractured surface of the ZrO_2:MgO pellet prepared by the coprecipitation technique.

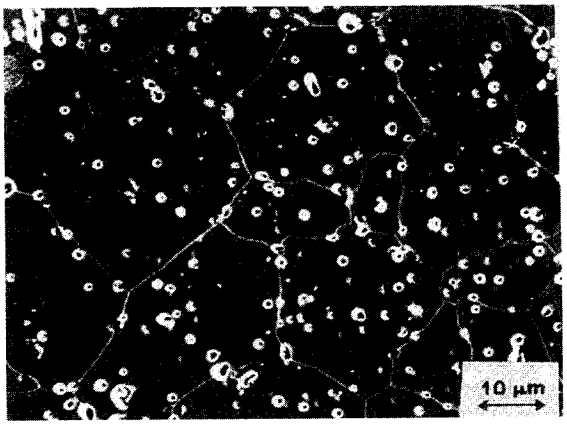

Fig. 4: SEM micrograph of a polished and thermally etched surface of the ZrO_2:MgO pellet prepared by the powder mixing technique.

The electrical resistivity (ρ) of ceramic materials are strongly affected by impurity elements. An increase in the overall resistivity when impurities segregate at the grain boundaries is usually found. Impedance spectroscopy is a powerful technique to study this effect in ceramic specimens because it allows for separating the contributions of grains and grain boundaries to the total resistivity. Fig. 5 show impedance diagrams for specimens synthesized by coprecipitation (a) and powder mixing (b) techniques. The high frequency semicircle is related to the resistivity of grains.

The low frequency semicircle results from the blocking of charge carriers by the grain boundaries. This blocking effect is seen only for specimens prepared by powder mixing while for coprecipitated specimens it is negligible.

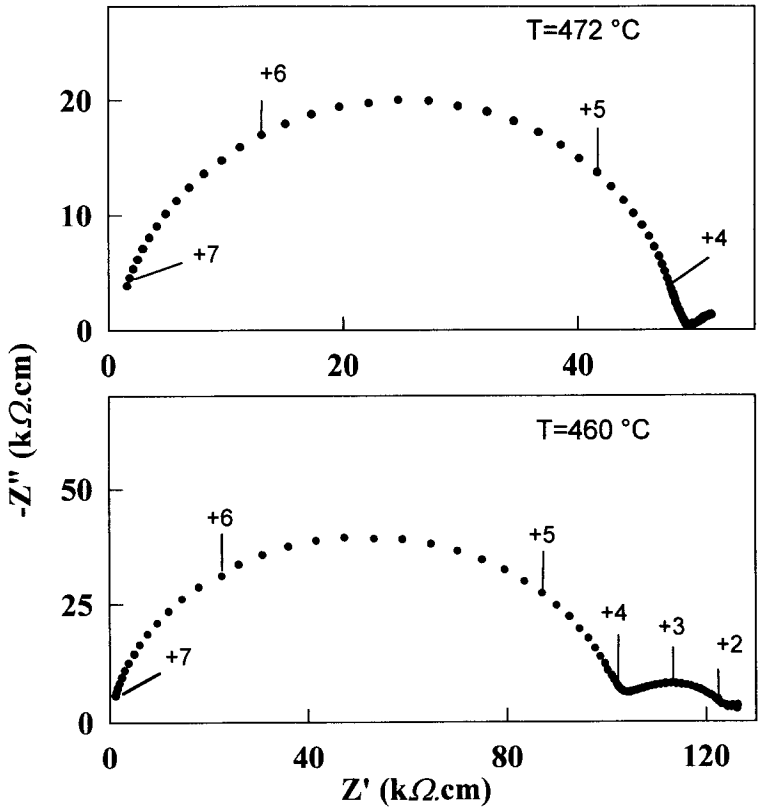

Fig. 5: Impedance diagrams of sintered zirconia-magnesia ceramics synthesized by coprecipitation (a) and powder mixing (b) techniques. Measurement temperature: (a) 472 °C, (b) 460 °C.

Resolution of these diagrams measured at different temperatures allows for obtaining the Arrhenius curves of the electrical resistivity (Fig. 6) for grains (g) and grain boundaries (gb). As depicted in this graph, the electrical resistivity of grains is lower for the coprecipitated specimen.

Values of conduction activation energies (E_g, E_{gb}), estimated resistivity (ρ^{1000}) at 1000 °C and dielectric constant (ε) are shown in Table 3.

Table 3: Values of activation energies for grains (E_g) and grain boundaries (E_{gb}), electrical resistivity at 1000 °C (ρ^{1000}) and dielectric constant (ε) for specimens synthesized by different techniques.

SPECIMEN	E_g (eV)	E_{gb} (eV)	ρ^{1000} (Ω.cm)	ε
ZM	1.32	-	7.67	46
DK-2	1.40	1.50	13.53	46

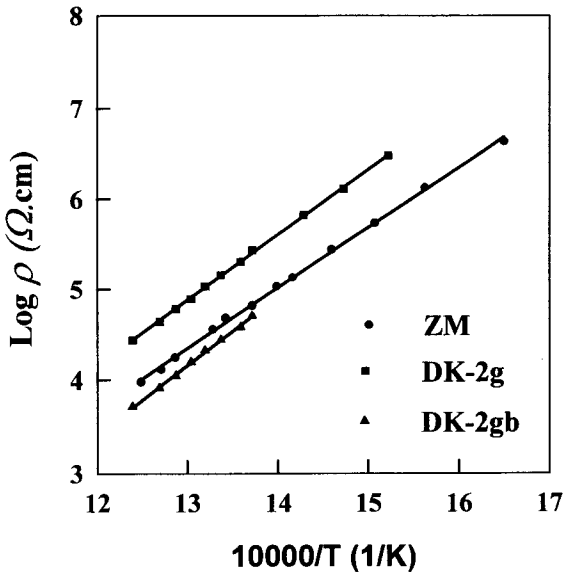

Fig. 6: Arrhenius plots of the electrical resistivity for specimens prepared by coprecipitation (ZM) and powder mixing (DK-2) techniques.

It is worth to note the difference in the values of the estimated resistivity. These results show that by careful processing of powders by chemical routes it is possible to obtain specimens of high purity quality and chemical homogeneity; thereby electrical properties can greatly be improved.

Zirconia-Ceria. Although many variables of the precipitation technique have been studied, for the sake of brevity only few results will be shown. Table 4 shows the metallic impurity content of starting materials. Si, Al and Mg are found in a relatively high concentration. These elements are known to be responsible for liquid phase sintering of this system and resulting secondary glassy phase formation at grain boundaries.

Table 4: Metallic impurity content (in wt.%) determined by inductively coupled plasma.

ELEMENT	$ZrOCl_2.8H_2O$	$Ce(NO_3)_3.6H_2O$
Si	0.03	0.15
Al	0.005	0.03
Mg	>0.02	<0.0045
Ca	-	0.03

Thermogravimetric results for the dried precipitate are shown in Fig. 7. The mass loss up to 600 °C is 21% and beyond this temperature it is negligible. These results are in agreement with those obtained previously [5].

Chloride content determined by pyrohydrolisis of the calcined powder was 35 ppm showing that the employed washing cycle was efficient for reducing this anion impurity to a low level.

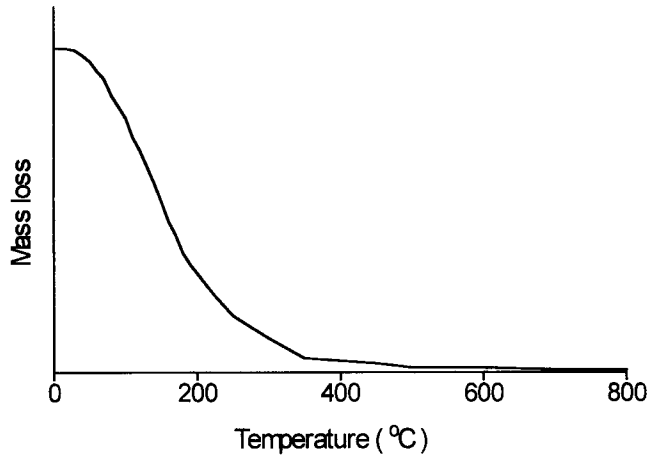

Fig. 7: Thermogravimetric curve of the zirconia-ceria powder.

Fig. 8 is a SEM micrograph of the calcined powder. As can be seen, large porous agglomerates are formed. In the subsequent pressing and sintering these agglomerates have proved to be soft.

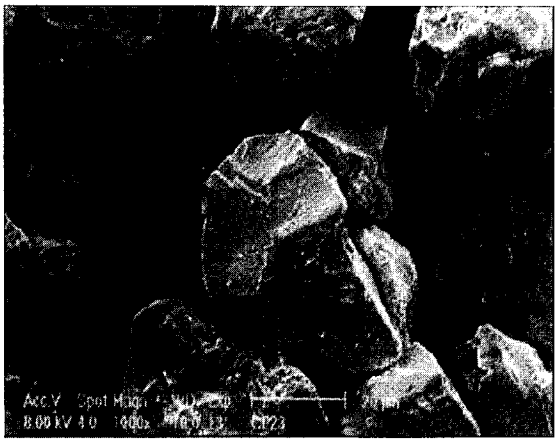

Fig. 8: SEM micrograph of the calcined zirconia-ceria powder.

X-ray diffraction results for the sintered ceramic are shown in Fig. 9. Only the main diffraction peaks for the tetragonal phase are seen showing total stabilization of this phase for this nominal ceria concentration. Lattice parameters determined in the usual manner using Si as standard, are shown in Table 5 along with other physical properties. These values are in agreement with results obtained in other works for the same nominal ceria content [11,12].

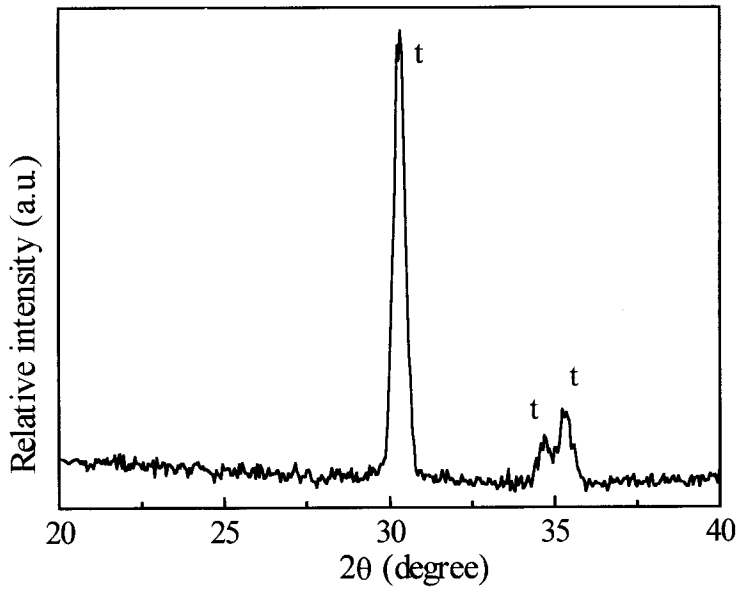

Fig. 9: X-ray diffractogram of the zirconia-ceria sintered specimen.

The sintered density reached 98% of the theoretical value without using any comminution or special drying processes. This result can be ascribed to the optimization of the synthesis parameters.

Table 5: Physical properties and experimental values for the zirconia-ceria specimen. TD: theoretical density.

Green density (% TD)	37
Hydrostatic density (% TD)	98
Tetragonal phase content (%)	100
Lattice parameters (nm)	
a	0.513(1)
c	0.525(8)

Fig. 10 is a SEM micrograph showing the fractured surface of the zirconia-ceria specimen. Relative low porosity and uniform grain size are the main microstructural features. From the grain size distribution an average value of 500 nm was determined.

Summary

High purity samples of zirconia-magnesia have been prepared by the coprecipitation technique. The same technique of synthesis has been used to produce zirconia-ceria ceramic powders with high sinterability. These results show that the optimization of the variables involved in this synthesis technique play a major role for obtaining zirconia-based ceramics with improved electrical and microstructural characteristics.

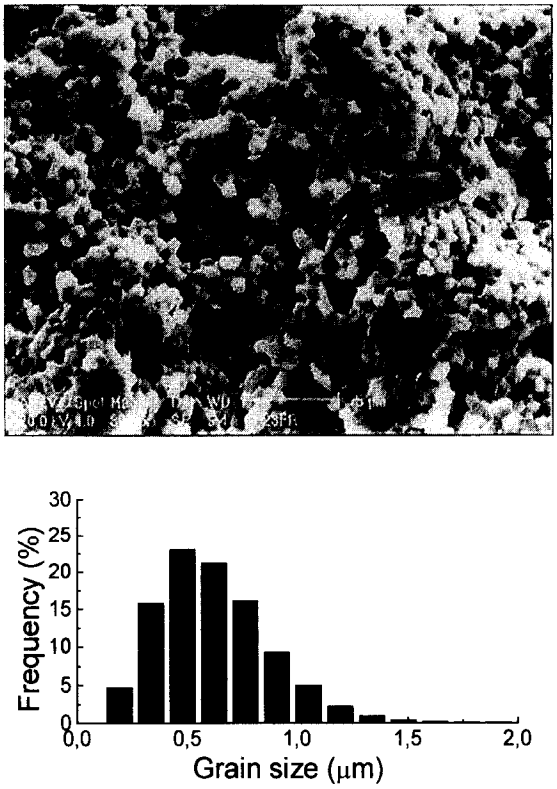

Fig. 10: SEM micrograph of a fractured surface and grain size distribution of the zirconia-ceria specimen.

Acknowledgements

To C. A. S. Queiroz, C. V. Morais, N. A. M. Ferreira, M. H. Carvalho, K. F. Portella and A. H. A. Bressiani. To Zirconia Sales for providing the ZrO_2 DK-2 type sample. To CNEN, FAPESP and PADCT-TR for financial support.

References

[1] D. W. Johnson, Jr. In *Ceramic Powder Science* (Adv. Ceram. **21**), ed. G. L. Messing, K. S. Mazdiyasni, J. W. McCauley, R. A. Haber. The Am. Ceram. Soc., Westerville, OH, 1987, p. 3.
[2] H. J. Stöcker. Ann. Chim. **5** (1960) p. 1459.
[3] D. R. Spink, J. H. Schemel. J. Nucl. Mater. **49** (1973) p. 1.
[4] T. Y. Tseng, C. C. Lin, J. T. Liaw. J. Mater. Sci. **22** (1987) p. 965.
[5] D. M. Ávila, E. N. S. Muccillo. Thermochim. Acta **256** (1995) p. 391.
[6] M. A. C. G. van de Graaf, K. Keizer, A. J. Burggraaf. Sci. Ceram. **10** (1979) p. 83.
[7] F. F. Lange. J. Am. Ceram Soc. **67** (1984) p. 83.
[8] J.-L. Shi, J.-H. Gao, T.-S. Yen. J. Am. Ceram. Soc. **74** (1991) p. 994.
[9] J. L. Shi, Z. X. Gao, Z. X. Lin, D. S. Yan. J. Mater. Sci. **28** (1993) p. 342.
[10] D. M. Ávila, E. N. S. Muccillo. J. Mater. Sci. Lett. **16** (1997) p. 685.
[11] K. Tsukuma, M. Shimada. J. Mater. Sci. **20** (1985) p. 1178.
[12] J.-G. Duh, H.-T. Dai, W.-Y. Hsu. J. Mater. Sci. **23** (1988) p. 2786.

Advanced Powder Technology I
doi:10.4028/www.scientific.net/MSF.299-300

Synthesis of Zirconia-Based Solid Electrolyte Powders by the Coprecipitation Technique
doi:10.4028/www.scientific.net/MSF.299-300.70